LETTERS

Local migration promotes competitive restraint in a host–pathogen 'tragedy of the commons'

Benjamin Kerr[1], Claudia Neuhauser[2], Brendan J. M. Bohannan[3] & Antony M. Dean[2]

Fragmented populations possess an intriguing duplicity: even if subpopulations are reliably extinction-prone, asynchrony in local extinctions and recolonizations makes global persistence possible[1–8]. Migration is a double-edged sword in such cases: too little migration prevents recolonization of extinct patches, whereas too much synchronizes subpopulations, raising the likelihood of global extinction. Both edges of this proverbial sword have been explored by manipulating the rate of migration within experimental populations[1,3–6,8]. However, few experiments have examined how the evolutionary ecology of fragmented populations depends on the pattern of migration[5]. Here, we show that the migration pattern affects both coexistence and evolution within a community of bacterial hosts (*Escherichia coli*) and viral pathogens (T4 coliphage) distributed across a large network of subpopulations. In particular, different patterns of migration select for distinct pathogen strategies, which we term 'rapacious' and 'prudent'. These strategies define a 'tragedy of the commons'[9]: rapacious phage displace prudent variants for shared host resources, but prudent phage are more productive when alone. We find that prudent phage dominate when migration is spatially restricted, while rapacious phage evolve under unrestricted migration. Thus, migration pattern alone can determine whether a *de novo* tragedy of the commons is resolved in favour of restraint.

Biological communities are often fragmented into subpopulations that are loosely linked through migration[10]. The dynamics of such 'metapopulations' have been investigated using theoretical models, statistical tools, field studies and laboratory experiments[10–13]. While extremely valuable, experiments with multi-species metapopulations have focused on ecological dynamics (for example, abundance data) in relatively small networks. The experimental evolution of interacting species in large metapopulations remains comparatively unexplored.

Using a model host–pathogen system[14–17], we investigated how the pattern of migration within large metapopulations affects eco-evolutionary dynamics. The bacterial host (*E. coli*) and its viral pathogen (T4) were embedded in 96-well microtitre plates, which imposed a metapopulation structure: each media-filled well was a subpopulation nested within the larger collection. The entire metapopulation was perpetuated through serial transfer, with each well culture diluted into a well with fresh medium every 12 h. At each transfer, migrations between wells were executed by a high-throughput liquid-handling robot according to a pre-specified migration scheme.

Our system illustrates the duplicitous nature of metapopulations. Empirically we find that bacteria and phage cannot coexist within a single well. However, our empirically calibrated simulations predict that coexistence in the metapopulation is feasible (see Box 1 and Fig. 1a, b). Wells come in three varieties (bacteria-filled, phage-filled and empty/media-filled) and exhibit a kind of 'rock–paper–scissors' dynamic: Migrating phage 'beat' bacteria (through infection and decimation), migrating bacteria 'beat' empty wells (through colonization), and empty wells 'overtake' phage (without host, phage are diluted to extinction). Spatially restricted migration leads to clumping of well types (Fig. 1c), which indicates spatial synchrony at small scales. The spatial asynchrony at large scales, which leads to the dampening of inherent oscillatory dynamics (compare Fig. 1a and Fig. 1b), is due to the decay of autocorrelations over space inherent to restricted

Box 1 | Empirically calibrated stochastic cellular automata

Each well in the metapopulation can be characterized as being in one of five discrete states: (1) filled with bacteria (state B), (2)–(4) filled with phage at one of three titres (decreasing from states P1 to P2 to P3) and no bacteria or (5) empty (state E). Even with abundant host, phage below the P3 titre have insufficient reproduction to compensate for dilution, and are thus effectively extinct. We empirically determine how each of these well states is transformed under dilution and migration events (see Methods). Collecting this information on single well transformations into a transition matrix (see Box 1 Table 1), we can explore the dynamics of a large collection of wells using stochastic cellular automata.

In this simulation technique, each point in a lattice represents a single well in one of the five possible states. The states of all points at time t are represented by S_t. Randomly assigning one of the states B, P1 or E to each point produces S_0. For each time step, every point in S_t is updated synchronously according to the rules in Table 1 to produce S_{t+1}. Migration into any focal point occurs with probability m from a randomly chosen point in its 'neighbourhood'. The 'Restricted neighbourhood' is the set of points directly north, south, east and west of the focal point (we employ wrap-around boundaries to avoid edge effects). The 'Unrestricted neighbourhood' is the set of all points in the lattice, minus the focal point. In Supplementary Information III we relate our stochastic cellular automata to another approach, the configuration field approximation.

Box 1 Table 1 | The transition matrix for states of wells

Current state	Future state				
	Bacteria (B)	Phage 1 (P1)	Phage 2 (P2)	Phage 3 (P3)	Empty (E)
Bacteria (B)	B, E, ∅	P1, P2, P3	NA	NA	NA
Phage 1 (P1)	NA	B	P1, P2, P3, E, ∅	NA	NA
Phage 2 (P2)	NA	B	P1	P2, P3, E, ∅	NA
Phage 3 (P3)	NA	B	P1	P2	P3, E, ∅
Empty (E)	B	NA	P1	P2	P3, E, ∅

All entries in this table give the identity of the state of the source well of migration that allows a focal well to transition from the relevant row state to the relevant column state. A well in state B has approximately 3.0×10^7 bacterial cells ml^{-1}, a well in state P1 has more than 3.0×10^7 phage ml^{-1}, a well in state P2 has between 3.0×10^6 and 3.0×10^7 phage ml^{-1}, a well in state P3 has between 3.0×10^5 and 3.0×10^6 phage ml^{-1}, and state E corresponds to a well with no bacteria and fewer than 3.0×10^5 phage ml^{-1}. The symbol ∅ refers to transitions in which there is no migration event (just a straight dilution of a focal well followed by incubation). NA, transitions that cannot occur.

[1]Department of Biology, University of Washington, Box 351800, Seattle, Washington 98195-1800, USA. [2]Department of Ecology, Evolution and Behaviour, University of Minnesota, 100 Ecology, 1987 Buford Circle, St Paul, Minnesota 55108, USA. [3]Department of Biological Sciences, Stanford University, Stanford, California 94305, USA.

migration. With spatially restricted migration, only phage at the boundaries between phage clumps and bacterial clumps can access fresh host. Relative to unrestricted migration, this limitation on host access is predicted to reduce the average phage density and increase the average bacterial density (compare Fig. 1a and Fig. 1b).

We tested these theoretical predictions using experimental metapopulations of 192 subpopulations (two 96-well plates) propagated by serial transfer on a 12-h cycle. Immediately after transfer, each metapopulation was exposed to one of three migration treatments. In the 'Restricted' treatment, migration into a focal well occurred from one of the north, south, east or west neighbours with probability $m = 0.45$ (we used 'wrap-around' boundaries so that every well had four neighbours). In the 'Unrestricted' treatment, migration into a focal well occurred from one of any other well in the metapopulation with the same probability, $m = 0.45$ (see Supplementary Information IV for the rationale behind this choice of migration probability, as well as more specific theoretical predictions). Although they varied with regard to the pattern of migration, both Restricted and Unrestricted treatments imposed some degree of population structure. In the 'Well-Mixed' treatment, all population structure was destroyed every 12-h cycle by thoroughly mixing the entire metapopulation in a large reservoir and then redistributing the mixture into a fresh set of wells. Each treatment was run for 20 cycles and replicated four times.

Consistent with theoretical predictions, we observed that population structure is critical to coexistence. The Well-Mixed treatment lost both bacteria and phage, whereas both types persisted in the other treatments (see Fig. 2a, b). Population instability was gauged by the coefficient of variation (CV) in phage or bacterial abundance over all time points. By this measure, bacteria in the Restricted treatment were more stable than in the Unrestricted treatment, although not significantly so ($\overline{CV}_{\text{Restricted}} = 0.951$, $\overline{CV}_{\text{Unrestricted}} = 1.276$, $P = 0.2$). Phage in the Restricted treatment were significantly more stable than in the Unrestricted treatment ($\overline{CV}_{\text{Restricted}} = 0.572$, $\overline{CV}_{\text{Unrestricted}} = 0.884$, $P = 0.02857$). Thus, restricted migration tends to stabilize community dynamics, as predicted by our simulations. In contrast to our predictions, we found no significant differences across treatments in average bacterial density ($\overline{N}_{\text{Restricted}} = 4.18 \times 10^7$, $\overline{N}_{\text{Unrestricted}} = 4.03 \times 10^7$, $P = 0.89$) or in average phage density ($\overline{N}_{\text{Restricted}} = 2.5 \times 10^8$, $\overline{N}_{\text{Unrestricted}} = 2.76 \times 10^8$, $P = 0.34$). What might account for this discrepancy?

The early appearance of resistant bacteria in the Unrestricted treatment might lower phage density below predicted values. However, appreciable resistance appeared only at the end of the experiment and did not differ in frequency between the treatments. As further evidence against the role of host evolution, bacterial isolates from the last transfer of each treatment did not differ in fitness from their common ancestor (see Supplementary Information I). By contrast, a stable polymorphism was evident in the phage after only a few transfers (see Supplementary Information II). Could evolution in the phage (rather than its bacterial host) lead to a relatively lower average phage density in the Unrestricted treatment?

To explore this possibility, we sampled four random phage isolates from the last transfer of each replicate and determined their productivities (number of phage produced per parent). Regardless of the initial multiplicity of infection (MOI, or ratio of phage to bacteria), phage from the Unrestricted treatment were significantly less productive than phage from the Restricted treatment (Fig. 2c). Hence, evolution in the phage accounts for the failure of our earlier ecological prediction.

Why would phage evolve lower productivity? At each MOI, phage from the Unrestricted treatment were significantly more competitive than phage from the Restricted treatment (in competition with a common 'marked' phage strain, see Methods and Fig. 2d). Moreover, a negative correlation between phage productivity and competitive ability was found at all three MOI levels and was significant in two cases (Kendall's test: low MOI $\tau = -0.25$, $P = 0.04545$; intermediate MOI $\tau = -0.1411$, $P = 0.2655$; high MOI $\tau = -0.4355$, $P = 0.00033$). This suggests that the evolution of higher competitive ability led to lower productivity.

These findings are consistent with a 'tragedy of the commons'[9], a scenario that arises when multiple users exploit the same resource. As

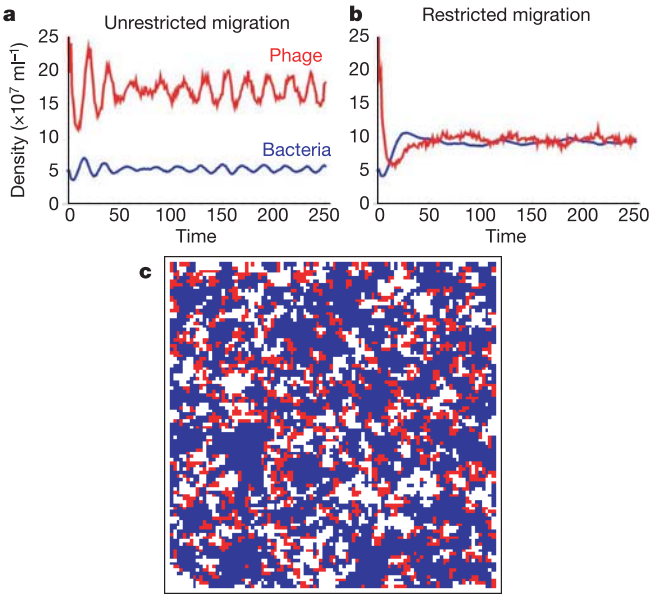

Figure 1 | Stochastic cellular automata predictions. The global densities of bacteria and phage on a lattice of 100 × 100 wells with an 'Unrestricted' migratory neighbourhood (**a**) and a 'Restricted' neighbourhood (only the north/south/east/west wells around a focal well can serve as sources of migration) (**b**). The migration probability is $m = 0.45$ in both cases. **c**, A snapshot of the Restricted neighbourhood lattice from time step 100, showing the clumping of bacteria-filled wells (blue), phage-filled wells (red) and empty wells (white).

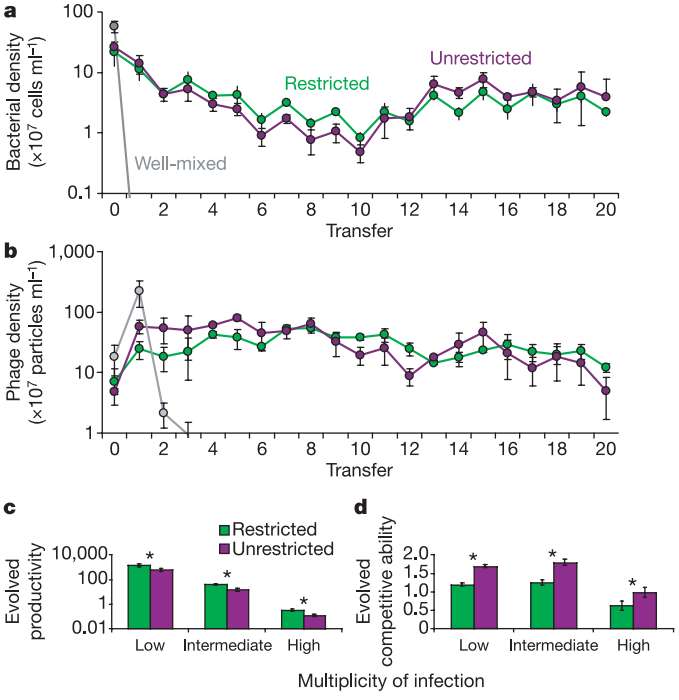

Figure 2 | Ecological and evolutionary results for experimental metapopulations. **a**, Average bacterial density and **b**, average phage density through time for each of the three treatments. **c**, Productivity and **d**, competitive ability of evolved phage at three multiplicities of infection. We plot mean ± s.e.m. and asterisks denote significance at the $P = 0.05$ level.

unrestrained users displace restrained competitors, the resource (the 'commons') is over-exploited, lowering overall user productivity (the 'tragedy'). The bacteria in each well are a common resource for resident phage. Prudent use of this resource leads to higher productivity of the phage (for example, if phage lengthen the time spent within a host before lysis, then uninfected hosts may continue to replicate, ensuring extended resource access). As shown by Abedon *et al.*[14], rapacious phage can out-compete their prudent cousins by limiting future access to the host through their own rapid host consumption. The 'tragedy of the commons' is that rapacious types lower overall productivity as they displace more restrained competitors.

Any rapacious phage mutant should displace its ancestor and lower overall productivity of its well. Given periodic dilution, however, less-productive phage subpopulations run a higher risk of extinction. The success of rapacious phage therefore depends on gaining sufficient access to fresh host to compensate for lower productivity. Such access is ensured by unlimited migration in the Unrestricted treatment. By contrast, spatially restricted migration reduces the probability that phage reach fresh hosts, rendering rapacious subpopulations more prone to extinction through dilution. Consequently, the tragedy of the commons is circumvented at the metapopulation scale in the Restricted treatment.

We claim that phage in our experimental metapopulations followed different evolutionary trajectories because of the pattern of migration. One potential concern is that phage under unrestricted migration may experience more replication owing to greater host access. Perhaps phage evolving under restricted migration did not have a sufficient number of generations (or 'doublings') for competitive variants to arise through mutation and displace their ancestors. Yet we find that the number of phage generations over the entire run, T, does not differ between the two treatments ($\overline{T}_{\text{Restricted}} = 64.7, \overline{T}_{\text{Unrestricted}} = 64.6$, $P = 1$, see Supplementary Information I). Evidently, lower evolved productivity and greater access to hosts in the Unrestricted metapopulation are balanced such that phage in both treatments experience a similar amount of replication. Hence, phage in the Restricted metapopulation had ample replication to evolve higher levels of competitiveness had there been universal selection for it.

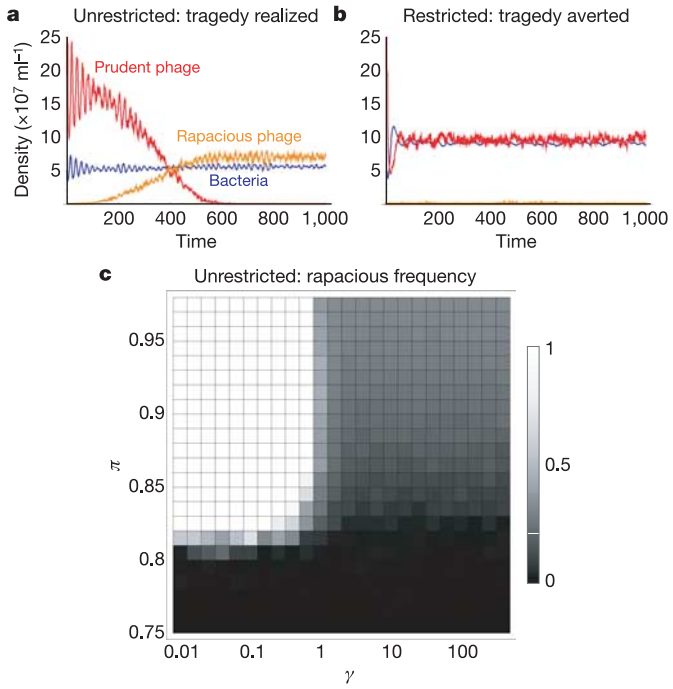

Figure 3 | Evolutionary stochastic cellular automata. In mixed subpopulations, rapacious phage out-compete prudent cohabitants with probability $\beta > 0$, but enter sub-critical levels one dilution earlier with probability $(1 - \pi) > 0$ (π is a measure of productivity/persistence). Let $\beta = (1 - \pi)^{\gamma}$ specify the trade-off between competitive ability and persistence (γ specifies the shape of the trade-off). The fate of rapacious phage (introduced by mutation into a 100×100 lattice with bacteria and prudent phage with $m = 0.45$, $\pi = 0.87$ and $\gamma = 0.1$) is shown given unrestricted (**a**) and restricted (**b**) migration. **c**, The frequency of phage that is rapacious after 3,000 cycles is shown on a greyscale for a number of different parameter combinations (each square is the average rapacious frequency over five simulation runs). With unrestricted migration, rapacious phage that are sufficiently persistent (large π) completely displace prudent types if the trade-off is sufficiently concave (small γ). None of the parameter combinations shown allows rapacious phage to persist at high frequencies given restricted migration.

Keeling[18] constructed a metapopulation model where short-term reproductive capacity of a pathogen trades off with long-term persistence. In agreement with his theoretical predictions, we demonstrated empirically that long-term strategies are favoured when dispersal between subpopulations is restricted. Similar trade-offs appear in the evolution of virulence literature[20–30], where virulence (defined here as an increase in host mortality due to infection) is assumed to covary with transmission[21,24–28] or competitive ability[18,20,23,28]. In our system, wells can be thought of either as microbial subpopulations or as multi-cellular hosts. From this second perspective, the rapacious strain is more virulent because the 'well host' dies sooner (that is, through dilution a less-productive strain goes extinct earlier), resulting in a trade-off between virulence and competitive ability. Assuming this or similar trade-offs, many researchers have investigated the role of host population structure on the evolution of virulence[2,18,20–22,25–27,29,30]. In our experiment, we control the social network of 'well hosts' through different migration treatments. Both our results and theory[18,21,25,29] suggest that highly connected social networks (for example, our Unrestricted treatment) favour virulence. Thus, network topology (between individuals or subpopulations) may profoundly influence the evolutionary trajectory of host–pathogen interactions.

Host–pathogen relationships are just one kind of victim–exploiter interaction, an ubiquitous category that includes prey and their predators and plants and their herbivores. Our results could apply to other victim–exploiter interactions embedded within metapopulations. Specifically, restricted migration between subpopulations may promote the evolution of prudent predation or restrained consumption. In general, restraint in the use of a common resource is a form of cooperation[19], and we have shown that spatial restrictions in migration within a metapopulation can favour relatively cooperative use of the common resource, thus averting the tragedy of the commons.

METHODS

Detailed methods and statistical analyses are available in Supplementary Information I.

Strains and media. We used the virulent bacteriophage T4 and *E. coli* B strain REL606 ($\text{Strep}^{R}\,\text{Nov}^{R}\,\text{T4}^{S}$), both grown in minimal glucose media supplemented with streptomycin and novobiocin. For the competition assay, we used an rII mutant strain of T4 (ATCC #11303-B40) to which *E. coli* K-12 λ-lysogen (ATCC #31278) is resistant, but REL606 is sensitive.

Well state transitions. The state of any well can be classified as follows: 'Bacteria' ($B \approx 3.0 \times 10^7$ cells ml^{-1} and $< 3.0 \times 10^5$ phage ml^{-1}), 'Phage 1' ($P1 > 3.0 \times 10^7$ phage ml^{-1}), 'Phage 2' ($3.0 \times 10^6 < P2 < 3.0 \times 10^7$ phage ml^{-1}), 'Phage 3'

($3.0 \times 10^5 <$ P3 $< 3.0 \times 10^6$ phage ml^{-1}), and 'Empty' (E has no bacteria and $<3.0 \times 10^5$ phage ml^{-1}). Even with abundant host, phage at subcritical titres (below P3) do not reproduce sufficiently and become extinct over successive dilutions. Bacteria persist in a well with subcritical levels of phage.

We determined a well-state transition in the following manner. A 'focal' well of a given state was diluted tenfold into a well with fresh medium (a 'target' well) and then a 'migrant' well of a given state was diluted approximately tenfold into the target well. After incubation for 12 h, we determined the state of the target well. Consider a table where the rows give the initial state of the focal well and columns give the final state of the target well (Box 1 Table 1). Each entry in this table is the state of the migrant well that yields the relevant row-to-column transition. The entry '∅' signifies a row-to-column transition due to dilution alone (that is, no migration). By empirically exploring all five initial states for the focal well and all six migration events (including the 'no migration' event ∅) we filled the Box 1 Table 1 ($5 \times 6 = 30$ entries give all possible transitions).

Experimental treatments. Each metapopulation consisted of two microtitre plates (192 wells, each with 200 μl growth medium). The initial spatial arrangement of well states was obtained from the 2,000th transfer of a 192-point lattice-based simulation with a Restricted neighbourhood. There were four replicates of each of three treatments: (1) Restricted, (2) Unrestricted and (3) Well-Mixed.

Every 12 h, we used a Biomek FX (Beckman-Coulter) liquid-handling robot with dual-pod action to execute all dilutions, migrations and transfers. Plates were incubated and shaken between transfers (550 r.p.m. on a microtitre shaker at 37 °C). We ran the experiment for a total of 20 transfers. One of the Unrestricted replicates was terminated after 16 transfers owing to contamination.

Isolating evolved phage strains. Using a soft-agar overlay with abundant *E. coli* K-12 λ-lysogen, we picked four random phage isolates (not rII mutants) from the last transfer of each of the Restricted and Unrestricted replicates (32 isolates in all).

Bacterial concentration for phage assays. When phage and bacteria are brought together through migration in the experimental metapopulations, there is an approximately tenfold dilution of both (migration immediately follows dilution). As a consequence, our phage assays are conducted using a tenfold dilution of the bacterial concentration that characterizes a well with fully grown bacteria (state B, see above). This concentration was chosen to mimic the conditions actually faced by the evolving phage.

Productivity assay. Each evolved T4 isolate was incubated for 12 h with approximately 3.0×10^6 REL606 cells ml^{-1} in a microtitre well. The initial and final titres of phage were used to estimate the productivity of the evolved phage (number of progeny produced per parent phage). Each evolved strain was assayed at three MOI levels (initial ratio of phage to bacteria) that mirror levels in the experiment: 'low' (0.05–0.2 MOI), 'intermediate' (0.5–4 MOI) and 'high' (5–60 MOI).

Competition assay. We mixed each evolved T4 isolate with rII phage in a 1:10 ratio inside a well with 3.0×10^6 REL606 cells ml^{-1}. Using the same three MOI levels, we measured phage titres before and after a 12-h incubation period. This was done by diluting and plating the mixture separately in overlays with *E. coli* K-12 λ-lysogen (only evolved isolates, not rII, form plaques) and *E. coli* REL606 (both evolved isolates and rII form plaques). The competitive ability of each evolved T4 relative to rII was calculated in one of the following ways:

(1) Per viral replication:

$$v(e,r) = \sqrt[D]{\frac{N_e(12)/N_e(0)}{N_r(12)/N_r(0)}}$$

(2) Per transfer:

$$u(e,r) = \frac{N_e(12)/N_e(0)}{N_r(12)/N_r(0)}$$

(3) Assuming continuous growth:

$$w(e,r) = \frac{\ln[N_e(12)/N_e(0)]}{\ln[N_r(12)/N_r(0)]}$$

where $N_e(t)$ and $N_r(t)$ are the densities of evolved T4 and rII, respectively, t hours after the assay begins. The parameter D gives the number of viral doublings that occurred over the assay. Where these measures yielded biologically reasonable values, they gave similar results (Fig. 2d uses the 'per viral replication' measure).

Received 12 March; accepted 4 May 2006.

1. Bonsall, M. B., French, D. R. & Hassell, M. P. Metapopulation structures affect persistence of predator–prey interactions. *J. Anim. Ecol.* **71,** 1075–1084 (2002).
2. Briggs, C. J. & Hoopes, M. F. Stabilizing effects in spatial parasitoid–host and predator–prey models: a review. *Theor. Popul. Biol.* **65,** 299–315 (2004).
3. Ellner, S. P. *et al.* Habitat structure and population persistence in an experimental community. *Nature* **412,** 538–543 (2001).
4. Holyoak, M. & Lawler, S. P. Persistence of an extinction-prone predator–prey interaction through metapopulation dynamics. *Ecology* **77,** 1867–1879 (1996).
5. Holyoak, M. Habitat patch arrangement and metapopulation persistence of predators and prey. *Am. Nat.* **156,** 378–389 (2000).
6. Huffaker, C. B. Experimental studies on predation: dispersion factors and predator–prey oscillations. *Hilgardia* **27,** 343–383 (1958).
7. Johst, K. & Schops, K. Persistence and conservation of a consumer-resource metapopulation with local overexploitation of resources. *Biol. Conserv.* **109,** 57–65 (2003).
8. Thrall, P. H., Godfree, R. & Burdon, J. J. Influence of spatial structure on pathogen colonization and extinction: a test using an experimental metapopulation. *Plant Pathol.* **52,** 350–361 (2003).
9. Hardin, G. The tragedy of the commons. *Science* **162,** 1243–1248 (1968).
10. Holyoak, M., Leibold, M. A. & Holt, R. D. *Metacommunities: Spatial Dynamics and Ecological Communities* (Univ. Chicago Press, Chicago, 2005).
11. Antonovics, J. in *Ecology, Genetics, and Evolution of Metapopulations* (eds Hanski, I. & Gaggiotti, O. E.) 471–488 (Elsevier, Oxford, 2004).
12. Grenfell, B., Bjørnstad, O. N. & Kappey, J. Travelling waves and spatial hierarchies in measles epidemics. *Nature* **414,** 716–723 (2001).
13. Keeling, M., Bjørnstad, O. N. & Grenfell, B. in *Ecology, Genetics, and Evolution of Metapopulations* (eds Hanski, I. & Gaggiotti, O. E.) 415–445 (Elsevier, Oxford, 2004).
14. Abedon, S. T., Hyman, P. & Thomas, C. Experimental examination of bacteriophage latent-period evolution as a response to bacterial availability. *Appl. Environ. Microbiol.* **69,** 7499–7506 (2003).
15. Bohannan, B. J. M. & Lenski, R. E. Linking genetic change to community evolution: insights from studies of bacteria and bacteriophage. *Ecol. Lett.* **3,** 362–377 (2000).
16. Lenski, R. E. & Levin, B. R. Constraints on the coevolution of bacteria and virulent phage: a model, some experiments, and predictions for natural communities. *Am. Nat.* **125,** 585–602 (1985).
17. Paddison, P. *et al.* The roles of the bacteriophage T4 r genes in lysis inhibition and fine-structure genetics: A new perspective. *Genetics* **148,** 1539–1550 (1998).
18. Keeling, M. Evolutionary trade-offs at two time-scales: competition versus persistence. *Proc. R. Soc. Lond. B* **267,** 385–391 (2000).
19. Kreft, J. U. Biofilms promote altruism. *Microbiology* **150,** 2751–2760 (2004).
20. Bergstrom, C. T., McElhany, P. & Real, L. A. Transmission bottlenecks as determinants of virulence in rapidly evolving pathogens. *Proc. Natl Acad. Sci. USA* **96,** 5095–5100 (1999).
21. Boots, M. & Sasaki, A. 'Small worlds' and the evolution of virulence: infection occurs locally and at a distance. *Proc. R. Soc. Lond. B* **266,** 1933–1938 (1999).
22. Bull, J. J., Molineux, I. J. & Rice, W. R. Selection of benevolence in a host–parasite system. *Evolution* **45,** 875–882 (1991).
23. Cooper, V. S. *et al.* Timing of transmission and the evolution of virulence of an insect virus. *Proc. R. Soc. Lond. B* **269,** 1161–1165 (2002).
24. Ebert, D. Virulence and local adaptation of a horizontally transmitted parasite. *Science* **265,** 1084–1086 (1994).
25. Galvani, A. P. Epidemiology meets evolutionary ecology. *Trends Ecol. Evol.* **18,** 132–139 (2003).
26. Herre, E. A. Population structure and the evolution of virulence in nematode parasites of fig wasps. *Science* **259,** 1442–1445 (1993).
27. Lipsitch, M., Herre, E. A. & Nowak, M. A. Host population structure and the evolution of virulence: a 'law of diminishing returns'. *Evolution* **49,** 743–748 (1995).
28. Nowak, M. A. & May, R. M. Superinfection and the evolution of parasite virulence. *Proc. R. Soc. Lond. B* **255,** 81–89 (1994).
29. O'Keefe, K. J. & Antonovics, J. Playing by different rules: The evolution of virulence in sterilizing pathogens. *Am. Nat.* **159,** 597–605 (2002).
30. Thrall, P. H. & Burdon, J. J. Evolution of virulence in a plant host–pathogen metapopulation. *Science* **299,** 1735–1737 (2003).

Supplementary Information is linked to the online version of the paper at www.nature.com/nature.

Acknowledgements We thank Y. Dang for help in the laboratory and the BioTechnology Resource Center at the University of Minnesota for robot access. We thank S. Abedon, C. Bergstrom, J. Bull, J. Fletcher, K. Koelle, C. Lehman, B. Levin and D. Stephens for useful feedback on this project and manuscript. This work was partially supported by an NSF grant to C.N. and an NIH grant to A.M.D.

Author Contributions B.K., A.M.D. and B.J.M.B. designed the experiments. B.K. and A.M.D. worked out the robotic protocols. B.K. programmed the robot, executed the experiments, and conducted the assays. B.K. and C.N. coded and analysed the empirically calibrated and evolutionary models. B.K., C.N. and A.M.D. conducted the statistical analysis. All authors contributed to the writing of the manuscript.

Author Information Reprints and permissions information is available at npg.nature.com/reprintsandpermissions. The authors declare no competing financial interests. Correspondence and requests for materials should be addressed to B.K. (kerrb@u.washington.edu).